Correlation between the Barcelona test and the bending test in fibre reinforced concrete

Eduardo Galeote[a, *], Ana Blanco[a], Sergio H.P. Cavalaro[a], Albert de la Fuente[a]

[a] Department of Civil and Environmental Engineering, Universitat Politècnica de Catalunya Barcelona Tech, Jordi Girona 1-3, C1, 08034 Barcelona, Spain

* Corresponding author: Eduardo Galeote. Department of Civil and Environmental Engineering, Universitat Politècnica de Catalunya Barcelona Tech, Jordi Girona 1-3, C1, 08034 Barcelona, Spain. Email address: eduardo.galeote@upc.edu

Abstract

The Barcelona test (BCN) is an alternative method to characterize the post-cracking behaviour of fibre reinforced concrete (FRC). Given its simplicity, the reduced scatter of the results and low material consumption, the BCN may represent a suitable method for the quality control of FRC. For that, a correlation between the results of the BCN and the bending test is currently required since the latter is considered the reference for the characterization of the material and for deriving the constitutive design equations. The objective of this paper is to propose such correlation following an approach that takes into account the intrinsic variability of FRC. An experimental program involving 21 mixes of conventional and self-compacting FRC with either steel or plastic fibres was performed. Several analyses were conducted both for selecting the most relevant parameters and for maximizing the degree of correlation between the tests. The highest correlation coefficient between tests was obtained for the mixes with plastic fibres. In

such case, the formulation proposed is able to predict the results with accuracy up to 75%. The correlation found is an interesting tool towards a simple and reliable quality control of FRC based on the BCN mainly oriented to large scale concrete production.

Keywords: correlation; fibre reinforced concrete; Barcelona test; flexural test; scatter

1 INTRODUCTION

The quality control of fibre reinforced concrete (FRC) used in structural applications should include tests for the assessment of the post-cracking response of the material. The selection of suitable testing methods for this purpose becomes particularly relevant given the high intrinsic scatter associated with the post-cracking response [1]. In this context, it is important to count with simple and fast methods that may provide enough repetitions for a reliable statistical analysis of the results that could lead to representative average and characteristic values of the post-cracking strength of the material.

The most extended method applied nowadays is the three-point bending test (3PBT) according to EN 14651:2007 [2]. It presents a coefficient of variation usually above 20% [3, 4] and a complex setup if compared to other tests, requiring special equipment and relatively big specimens. For these reasons, as suggested by the Belgian standard NBN B 15-238 [5], the 3PBT is not considered suitable for the systematic quality control of FRC. Thereby, alternative tests were developed in an attempt to overcome the drawbacks previously mentioned [6-8]. In this context, the *fib* Model Code 2010 [9] allows the use of alternative tests to obtain the residual strength of FRC if appropriately correlated to the results of the 3PBT. Therefore, in case such correlations are achieved, the substitution of the bending test by an alternative approach may be accepted.

The use of correlations between concrete properties measured in different test methods is a common and widely accepted procedure, even when the cracking mechanisms involved in each of them are completely different. For example, equations relating the compressive strength and the tensile strength are present in the majority of structural concrete codes and guidelines. Moreover, several equations are available to transform the indirect tensile strength measured in the Brazilian Test into the indirect flexural strength measured with bending tests [10]. In the case of FRC, Minelli et al. [11] already proposed a correlation between the Round Panel Test and the UNI flexural test based on the energy released and the residual strength. Correlations between different typologies of tests also provide an opportunity for developing new simplified stress-crack width laws for FRC [12, 13].

Another alternative to characterize the tensile residual strength of FRC is the Barcelona test (BCN) proposed by Molins et al. [4] and included in the standard UNE 83515:2010 [14]. Recently, it has been improved by Pujadas et al. [15, 16] and a constitutive equation based on the results of the test was proposed by Blanco et al. [17]. The BCN is simpler than the 3PBT in terms of execution since 75% lighter specimens are used and no closed-loop is required. It also presents smaller scatter [15] with a coefficient of variation of the results below 13% [4]. Despite these advantages, the use of the BCN for the characterization of FRC is hindered by the lack of correlations with the 3PBT.

Taking that into account, the objective of this paper is to correlate the results of both tests so the BCN may be used as a complementary method to characterize the properties of FRC. The approach presented here aims to obtain simple and reliable correlations taking into account the typical variability of the material. In this regard, the correlation proposed represents a tool towards a simpler, faster and less expensive quality control of FRC based on the BCN. This approach is in line with the *fib* Model Code 2010 and may also serve as an example for future correlations with other tests applied to FRC.

2 METHODOLOGY TO CORRELATE THE TESTS

The approach proposed to determine the correlation between the BCN and the 3PBT consists of three stages, as indicated in Fig. 1. In the first stage, an experimental program with a wide variety of concrete types was performed. In the second stage, linear regressions are performed considering different variables included in the study. This helps determining whether a universal correlation between both tests is possible or if different formulations are needed depending on the type of concrete, the type of fibre or the fibre content.

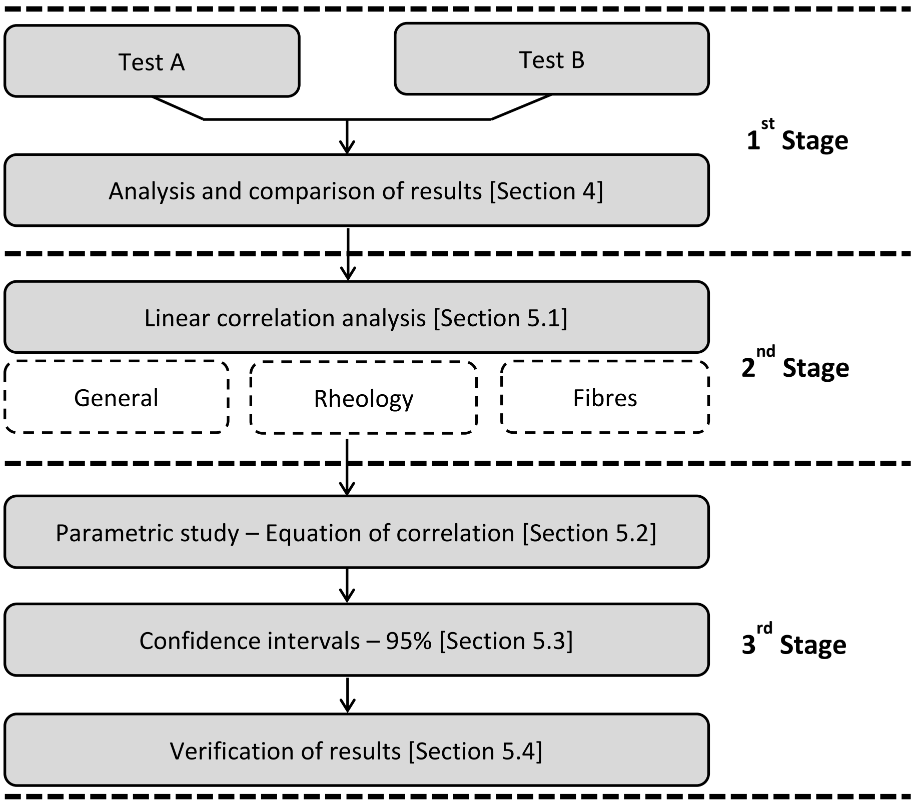

Fig. 1. Methodology used to derive the correlation between tests.

In the third stage a multi-variable parametric study is conducted in order to obtain the final correlations. To account for the variability of the FRC, an approach similar to that used in sprayed concrete is applied. Instead of proposing a single equation, a correlation zone defined by confidence intervals is derived through a statistical analysis of the results. Equations for the 50% and 95% confidence are proposed.

3 EXPERIMENTAL PROGRAM

3.1 Materials and mixes

Mixes with conventional concrete (CC) and self-compacting concrete (SCC) were produced. The flowability of concrete may influence the residual strength of FRC since it affects the orientation of the fibres [18-23]. In total, 21 concrete mixes were designed with water-to-cement ratios ranging from 0.19 to 0.56. Different types of cements were used, with total contents between 275 and 700 kg/m^3. Hooked-end steel fibres (SF) were added in contents from 30 to 60 kg/m^3, whereas the content of 3 types of plastic fibres (PF1, PF2 and PF3) varied from 3.5 to 25 kg/m^3.

Table 1 summarizes the mixes depending on the main variables of the study. The compressive strength in each mix is the average of 3 specimens of ϕ150x300 mm tested under compression according to EN 12390-3 [24]. The nomenclature includes the type of fibre and the content used. Table 2 shows the main characteristics of each type of fibre.

Rheology	***Strength Classificat.***	***Compressive Strength [MPa]***	***Fibre***		***Nomenclature***
			Type	***Content [kg/m^3]***	
Conventional concrete (CC)	>60 MPa	66.4	SF	30	CC_H60_SF_30
		65.1	SF	45	CC_H60_SF_45
		66.2	SF	60	CC_H60_SF_60
		85.0	PF3	25	CC_H60_PF3_25
	<60 MPa	47.7	PF1	4	CC_L60_PF1_4
		46.1	PF1	6	CC_L60_PF1_6
		48.1	PF1	8	CC_L60_PF1_8
		51.6	PF2	4	CC_L60_PF2_4
		52.9	PF2	6	CC_L60_PF2_6
		52.5	PF2	8	CC_L60_PF2_8
Self-compacting concrete (SCC)	>60 MPa	71.9	SF	30	SCC_H60_SF_30
		67.6	SF	45	SCC_H60_SF_45
		60.2	SF	50	SCC_H60_SF_50
		66.9	SF	60	SCC_H60_SF_60
		82.6	PF3	10	SCC_H60_PF3_10
		77.2	PF3	20	SCC_H60_PF3_20
	<60 MPa	50.1	SF	50	SCC_L60_SF_50A
		40.4	SF	50	SCC_L60_SF_50B
		34.4	SF	50	SCC_L60_SF_50C
		57.4	PF1	3.5	SCC_L60_PF1_3.5A
		52.4	PF1	3.5	SCC_L60_PF1_3.5B

Table 1. Main characteristics of the mixes.

Properties	***SF***	***PF1***	***PF2***	***PF3***
Material	Steel	Polypropylene	Polypropylene	Polyvinyl alcohol
Elastic Modulus [GPa]	500	4.0	4.8	8.5
Tensile strength [MPa]	1000	400	338	800
Length [mm]	50	48	40	12
Diameter [mm]	1.00	0.84	0.75	0.20
Aspect ratio [-]	50	57	53	60

Table 2. Fibres characteristics (data provided by the manufacturers).

3.2 Specimens and test procedure

As shown in Fig. 2, the BCN consists of a double punch test on a cylindrical (ϕ150 mm x 150 mm) or cubic (150 mm) specimen. The test is performed by placing, concentrically above and below the specimen, cylindrical steel punches with a height of 25 mm and a diameter equal to ¼ of the smaller dimension of the cross-section of the specimen. The hydraulic press applies a load to the punches at a constant displacement rate of 0.5 ± 0.05 mm per minute. In the process, a conical triaxial state is formed from the centre to the edges of the specimen, leading to internal tensile stresses that increase with the load. Cracks appear (Fig. 2) when the stresses reach the tensile strength of the concrete matrix. After that, the fibres bridge the crack, providing a residual strength. The results obtained may be represented through a Load-Total Circumferential Opening Displacement (TCOD) curve or Load-Axial Displacement relationship depending on the equipment used in the test, as depicted in Fig. 2.

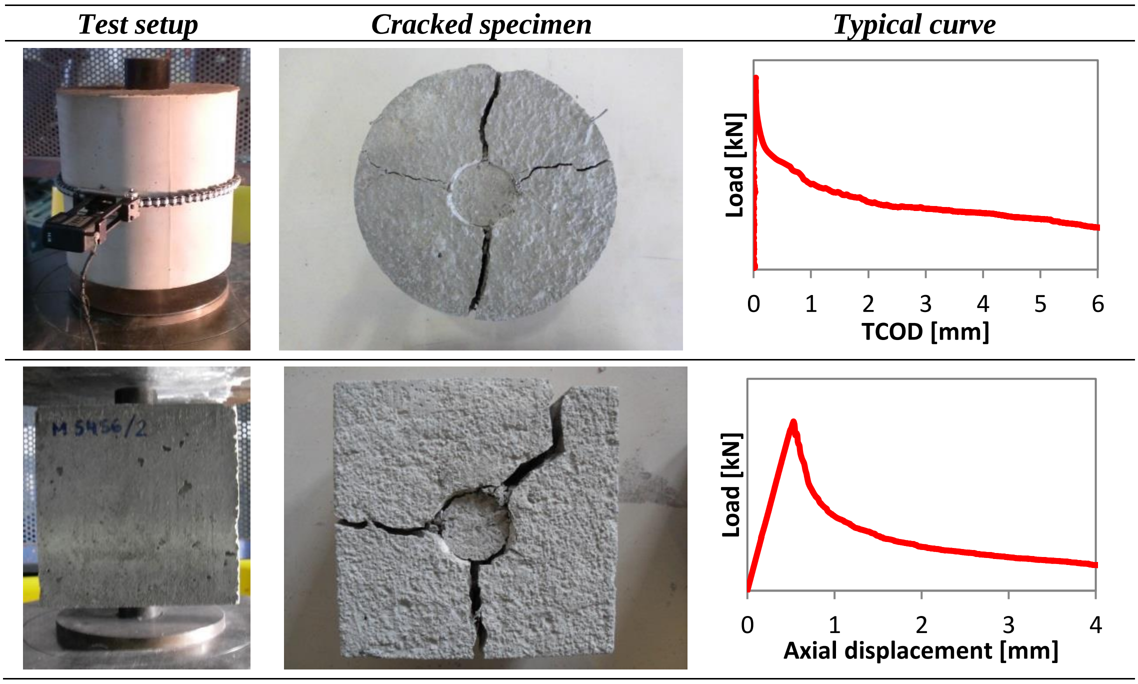

Fig. 2. BCN in cylindrical and cubic specimens.

The main difficulties to obtain acceptable correlations lay on the differences in the crack mechanism observed in both tests and, especially, the high variability intrinsic to the FRC. The fracture mechanism of the 3PBT is purely dominated by Mode I, while in the BCN the propagation of the crack is a mixed response between Modes I and II. This is shown in Fig. 3, which shows how the penetration of the two cones into the specimen (Mode II) produces the opening of several radial cracks where tensile stresses appear perpendicular to the fracture surface (Mode I).

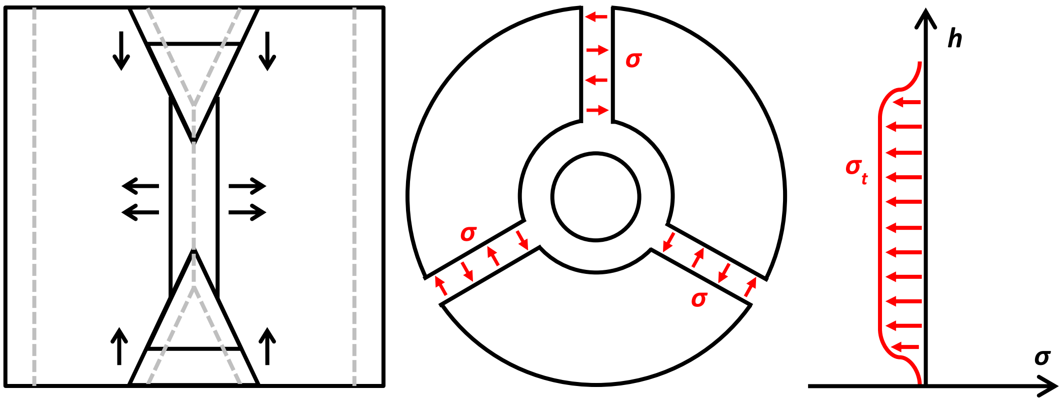

Fig. 3. Cracking mechanism and distribution of stresses.

Even though the failure mechanisms between 3PBT and the BCN might be different, this should not pose a problem to obtain a correlation between both tests. In fact, several codes and studies from the literature propose correlations between the results of test methods with completely different cracking mechanisms (for example, between compressive and tensile strength or between tensile and flexural strength, among others).

For all mixes produced here, 2 shapes of moulded specimens were manufactured: 72 beams of 150 x 150 x 600 mm for the 3PBT (according with the EN 14651:2007) and 72 cubes of 150 mm of side for the BCN. Once the 3PBT were concluded, each beam was cut in order to obtain 150 x 150 mm cubic specimens, resulting in 144 additional samples for the BCN test. As depicted in Fig. 4, these cuts were performed disregarding the first 50 mm from the extremities of the beam – in order to avoid the influence of the wall effect – and the central 200 mm – to avoid the influence of the crack produced during the 3PBT.

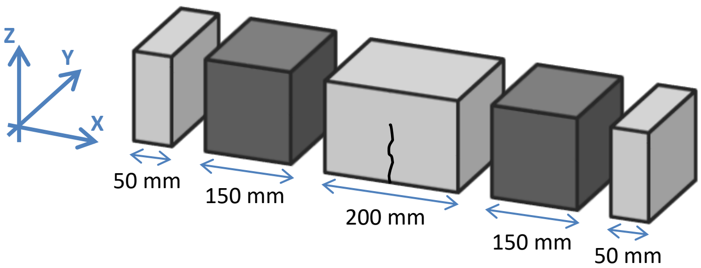

Fig. 4. Cubic specimens cut from the beams.

After that, the inductive test [25, 26] was conducted in moulded and cubic specimens with included steel fibres. In this test, a coil is used to measure the content and preferential orientation of the fibres in the axes perpendicular to the faces of the specimens. The convention from Fig. 4 was adopted. According to this convention, the Z-direction is always parallel to the concrete casting direction. In the cut specimens, the X-direction is parallel to the length of the beam. In moulded specimens, the directions X and Y are defined indistinctly since, in principle, no in-plane preferential direction is evident. Finally, the BCN (Fig. 2) was performed as described in this section in all cubic specimens. The direction of loading was parallel to the casting direction (Z). The force measured during the test was converted into stress following the equations proposed by [14].

4 ANALYSIS AND COMPARISON OF THE RESULTS

A preliminary analysis of the results is conducted to evaluate the influence of the variables from the study and the need to include them in the correlation. Even though other variables were also analysed, this section only describes the influence of the content of fibres, the rheology (conventional or self-compacting) and the type of cubic specimen (moulded or cut).

4.1 Influence of the fibre type

The differences between steel and plastic fibres in the mechanical response of FRC have been extensively described in literature [27-31] and are not the objective of this paper. Rather than that, the results of the 3PBT and the BCN for different contents of SF are compared. The influence of the contents is depicted in Fig. 5 in a plot Load-Crack Mouth Opening Displacement (CMOD) for the 3PBT and Load-Axial Displacement for the BCN results.

The results from the 3PBT and BCN show a similar variation with the fibre content. In other words, higher stresses are resisted as the fibre content increases. The strength obtained in the BCN is in general lower than the strength observed in the 3PBT. This was more remarkable in dosage SCC_H60_SF_60 with 60 kg/m^3 of fibres, which was the only one to present hardening in the 3PBT after the first crack appeared. Conversely, none of the dosages presented hardening behaviour in the BCN.

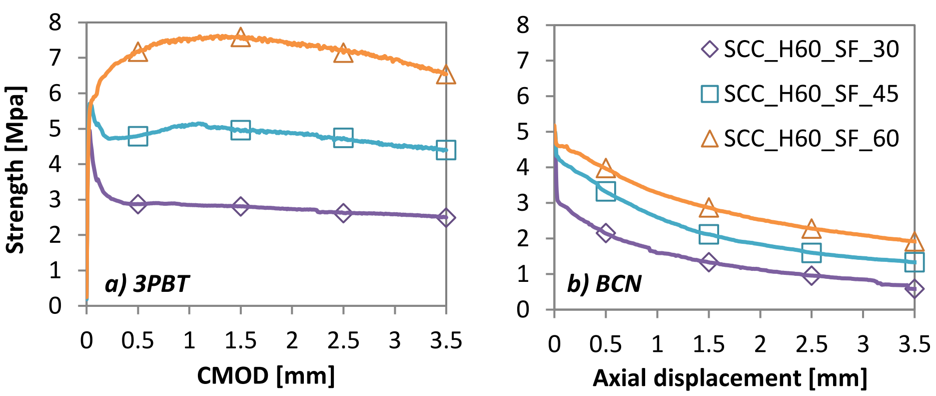

Fig. 5. Residual strength in a) 3PBT and b) BCN.

This outcome may be attributed to the differences between the cracking mechanisms in each test. Previous studies showed that the same FRC may present hardening in bending tests and softening in direct tension tests [32]. In the former, the crack length increases gradually due to the formation of a par with compression stresses provided by the unaffected concrete matrix and tensile stresses provided by the fibre bridging the cracks. Conversely, in the direct tension tests, the cracks tend to form abruptly, almost eliminating the contribution of the concrete matrix that has to be resisted by the fibres at this moment. In this context, a change of stiffness is more likely to occur, being observed as a drop in the stresses resisted just after cracking. Notice that the mechanism developed in the BCN is closer to that found in the direct tension test than in the bending test since cracks appear abruptly and the contribution of concrete is hindered.

Another factor that could explain the lower stresses found in the BCN in comparison with the 3PBT is the effective number and orientation of fibres bridging the cracks. In the BCN, between 2 and 4 cracks are formed during the test. Usually the cracks with lower contribution of fibre tend to open more than others with higher fibre contribution. Therefore, the stresses measured become influenced by the overall in-plane fibre orientation instead of being a result of a single cracking plane that tend to be perpendicular to the direction with higher contribution, such as in the 3PBT.

4.2 Influence of the rheology

Fig. 6 shows the average residual strengths measured with 13 specimens tested under the BCN and 3 specimens tested by means of the 3PBT for each of the two equivalent mixes of conventional and self-compacting concrete: CC_H60_SF_45 and

SCC_H60_SF_45, respectively. The scatter of the results is also shown using the coefficient of variation (CV) represented at the right vertical axis. Notice that both mixes present the identical nominal fibre type and content, as well as similar average compressive strength.

Immediately after cracking occurs in the 3PBT, the average residual strength of CC_H60_SF_45 is higher than that of SCC_H60_SF_45. As the crack opening grows, the trend is inverted and the performance of SCC_H60_SF_45 is greater than CC_H60_SF_45. By the typical scatter of the 3PBT, the results of the flexural test may be considered approximately the same. This conclusion is also derived from the analysis of the results from the BCN, which shows approximately the same residual strength for SCC_H60_SF_45 and SCC_H60_SF_45 throughout the test.

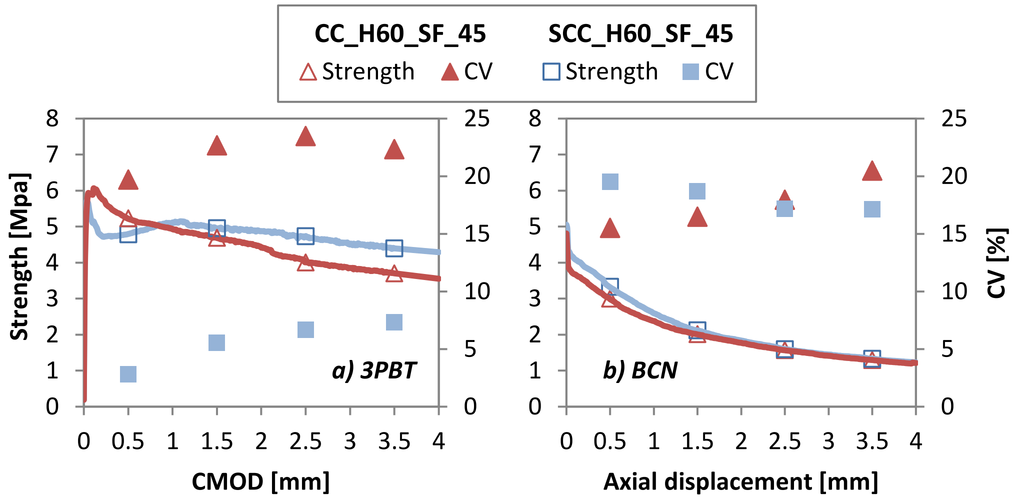

Fig. 6. Influence of the rheology in the results of the a) 3PBT and the b) BCN.

The similarities of the residual response of both types of concrete may be explained by the fibre orientation. In the specimens cut from the beams tested with the 3PBT, the contribution of fibres in the X-direction is 41.5% for conventional concrete and 43.2% for self-compacting concrete. It is evident that, in spite of the change in rheology, small variations in terms of fibre orientation are observed in the main direction characterized in this 3PBT. Likewise, the contribution of fibres in the plane XY in moulded specimens tested with the BCN is approximately 80% regardless of the type of concrete. All these results justify the similarities between conventional and self-compacting concrete assessed in this study.

4.3 Influence of the type of cubic specimen

The manufacturing procedure of the two types of cubic specimen (cast and cut from the beam) may affect both the orientation and the mechanical performance. For this reason, the fibre orientation and the mechanical performance of both types of specimen is assessed and compared in order to know whether they may be used indistinctly for the assessment of the correlation. Table 3 shows the average orientation measured with the inductive test and the corresponding coefficient of variation (CV) in both types of specimen calculated for the 10 dosages with different contents of steel fibres. Illustrative schemes of the preferential orientation measured are also presented.

Type of specimen	***X-axis***		***Y-axis***		***Z-axis***		***Scheme of orientation***
	Orientation	***CV***	***Orientation***	***CV***	***Orientation***	***CV***	
Cut	46.5%	5.6%	33.1%	7.0%	20.4%	6.9%	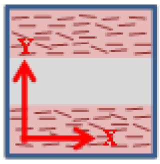
Moulded	38.9%	3.5%	38.9%	3.0%	22.2%	8.6%	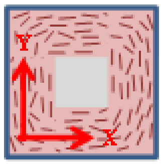

Table 3. Average values and CV of the fibre contribution for cut and moulded specimens.

Approximately 80% of the contribution of the fibres is concentrated in the plane perpendicular to the casting direction in both types of specimens. This may be explained by the flow and the external vibration applied in some of them during the production, which favour a fibre alignment parallel to the XY plane [18, 20, 33-35].

In cut specimens, 46.5% of the contribution of the fibres is concentrated in X while only 33.1% of the contribution is observed in Y. This contrasts with the results from the moulded specimens, which display almost the same contribution of fibres in X and in Y. Interestingly, the scatter for the measurements in both directions for cut specimens is around twice as high as the calculated for moulded specimens (see CV in Table 3).

All these differences may be attributed to the influence of the shape of the specimens, the wall-effect and the flow of concrete during the production process. In the case of the cut specimens, the predominant wall effect is observed along the X-direction of the beam. This is also the main flowing direction, favouring a higher fibre contribution in this direction. Nevertheless, in the case of moulded specimens, the wall-effect imposed by the formwork and the distance of flow in X and in Y should be practically identical. Consequently, similar contributions are observed.

The influence of the content of SF on the orientation of each type of specimen is exhibited in Fig. 7. As expected, the content of fibres showed no significant influence on the orientation. This is reasonable since the same mixing and casting process was used. Moreover, the trend in the orientation is similar to the previously described in Table 3.

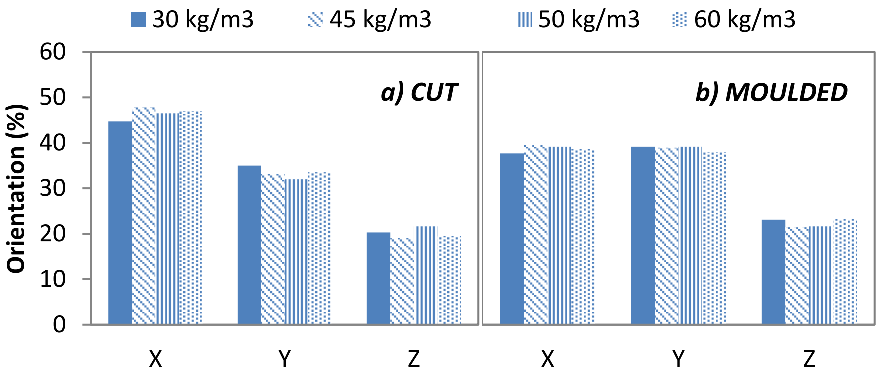

Fig. 7. Orientation of fibres according to the content in a) cut and b) moulded specimens.

Fig. 8.a and 8.b show the average residual strength for the dosages with 50 kg/m^3 of steel fibres (SCC_L60_SF_50A, SCC_L60_SF_50B, SCC_L60_SF_50C and SCC_H60_SF_50) and 3.5 kg/m^3 of plastic fibres (SCC_L60_PF1_3.5A and SCC_L60_PF1_3.5B), respectively. Other mixes present similar results. The grey curves show the average strength of each dosage depending on the type of specimen. The red curves represent the average strength of all dosages separated by cut or moulded samples.

No significant difference between the moulded and cut specimens was expected in the mechanical results since in both cases approximately 80% of the fibres are aligned in the XY plane. The curves confirm the small differences in terms of the average residual strength regardless of the type of fibre used. A slightly bigger scatter is observed in the cut specimens, which is in line with the higher CV found in the fibre contribution for the latter in Table 3. The results suggest that the average mechanical results obtained between moulded and cut samples are similar enough to use both types of specimens in the correlation analysis.

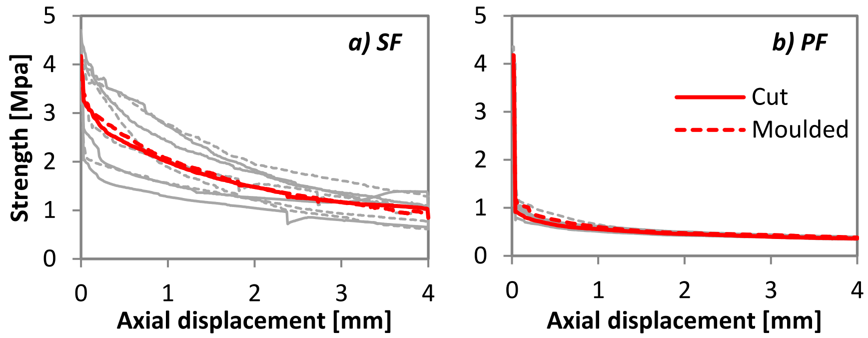

Fig. 8. Residual strength with BCN in cut and moulded specimens with a) SF and b) PF.

5 CORRELATIONS

5.1 Correlation depending on variables and test parameters

In this section a linear regression is performed between different parameters from the tests to identify those that provide the highest correlation degrees. Besides identifying the parameters that provide the best correlation, the aim is to determine whether a general correlation is possible or if it is necessary to derive specific formulations depending on the type of concrete or of fibre used.

The average stress and the average tenacity of each concrete mix were calculated for reference displacement values. For the 3PBT, the CMOD of 0.5, 1.5, 2.5 and 3.5 mm were taken as a reference. In the case of the BCN, the axial displacements of 0.5, 1.5, 2.5 and 3.5 mm from the beginning of the test and also after cracking were taken as a reference. The nomenclature used to refer to each parameter starts with the letter “F” for forces and “E” for energy values. Then, either “bcn” or “3pbt” is appended as a subscript depending on the test. The corresponding CMOD or axial displacement is placed at the end as a subscript. For example, $E_{bcn,1.5}$ represents the energy estimated in the BCN for an axial displacement up to 1.5 mm after cracking.

Correlations were performed with every possible combination of one parameter of the 3PBT and one parameter of the BCN. This procedure was repeated considering all data from the experimental program or by grouping the data by rheology (conventional or self-compacting concrete), by strength class (smaller than 60 MPa or bigger than 60) and type or content of fibre. To simplify the analysis of the results, the minimum, the maximum and the average correlation degrees were calculated for all possible combinations with each parameter of the BCN. Fig. 9 shows a summary of the coefficients of determination (R^2) obtained for $F_{bcn,0.5}$, $F_{bcn,1.5}$ and $E_{bcn,1.5}$, which were the parameters that showed the highest correlation degree in the linear correlation among all the analysed parameters. These represent the load and the energy obtained in the BCN for axial displacements of 0.5 and 1.5 mm measured after cracking.

The analysis shows a significant variability in R^2. When all data are considered, the average R^2 is approximately 0.60, represented in a dashed line in Fig. 9. This is also true for all correlations performed when the results are grouped by rheology. Notice that the average calculated for conventional concrete is the same as that for self-compacting concrete. This suggests that the results from both concrete types may be considered indistinctly in the same formulation without compromising R^2. Despite that, it is noteworthy that the scatter in R^2 is twice as high in the conventional concrete than in self-compacting concrete.

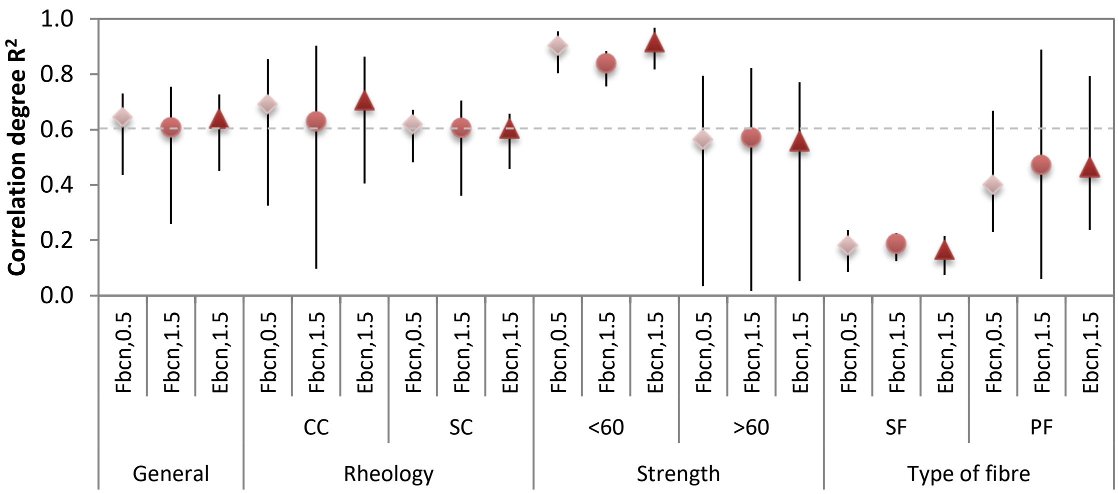

Fig. 9. Results of linear correlation analysis.

Significant differences are observed when the data is grouped by strength class. In the case of mixes with compressive strength below 60 MPa, average R^2 values close to 0.90 are obtained. This improvement with regards to the general correlation is compensated by a smaller average R^2 in the mixes with compressive strength above 60 MPa. Moreover, a higher variability is observed in this last group. Based on these results, the definition of separate correlations is not justified since the improvement observed would be minor.

The grouping by fibre type shows lower average values of R^2 for steel fibre than for plastic fibre. Such outcome may be attributed to the wider range of contents tested in the former, which varies from 3.5 to 25 kg/m³. This contrasts with the range of steel fibres that goes from 30 kg/m³ to 60 kg/m³. Despite the difference in terms of average values, the variability in the results of the R^2 calculated in plastic fibre is several times bigger, presenting values that are close to those of steel fibre.

It is important to remark that the average R^2 obtained after grouping the fibres by type is smaller than that of the general correlation. Again, this indicates that the separate consideration is not justified since it would not contribute to a better correlation in the case of the present experimental program. Therefore, a general correlation applicable to all types of concrete, types and contents of fibre is proposed in the next section.

5.2 Proposal of correlation

An in-depth analysis was performed to identify the equation that provides the best correlations between the BCN and the 3PBT. In order to increase R^2 values, a multivariable regression was performed. The outcome of the equation should be a parameter of the 3PBT, whereas the input should consist of parameters of the BCN or other characteristics of the concrete. After several regressions, it was found that the best correlations relate the force measured for a certain value of CMOD in the 3PBT with the force and the energy for the same axial displacement measured in the BCN. Eq. 1 shows the equation proposed as a result of the regression study.

$$F_{3PBT,i} = a \cdot F_{BCN,i} + b \cdot {E_{BCN,i}}^2 \qquad (1)$$

In this equation, the terms *a* and *b* are constants obtained in the regression for a CMOD and an axial displacement of *i*. The values of both constants and of the R^2 are presented in Table 4. The *i* corresponding to 0.5 mm is not included in the table since in this case it was not possible to identify an acceptable correlation between tests. This may be attributed to the differences in terms of crack formation in both tests, whose influence is evident for low displacements. This issue was also described by Bernard [36], who did not find good correlations between tests at low levels of deformation.

***i* (mm)**	***a***	***b***	**$CI_{99\%}$ (kN)**	**R**	**R^2**
1.5	1.76E-01	-3.29E-04	2.00	0.86	0.74
2.5	1.45E-01	4.70E-06	1.67	0.89	0.79
3.5	1.52E-01	1.46E-05	1.65	0.87	0.76

Table 4. Constants and confidence interval of Eq. 2.

Fig. 10 shows the comparison between the results obtained from 3PBT and the corresponding result estimated for the same mix with Eq. 1 from the results of the BCN for the displacements *i* of 1.5, 2.5 and 3.5 mm. The straight line indicates the equivalence line. The predictions made with Eq. 1 approaches the results from the 3PBT despite the wide variety of compositions and fibre types used. As the displacement increases, so does the goodness of the predictions made with the correlation.

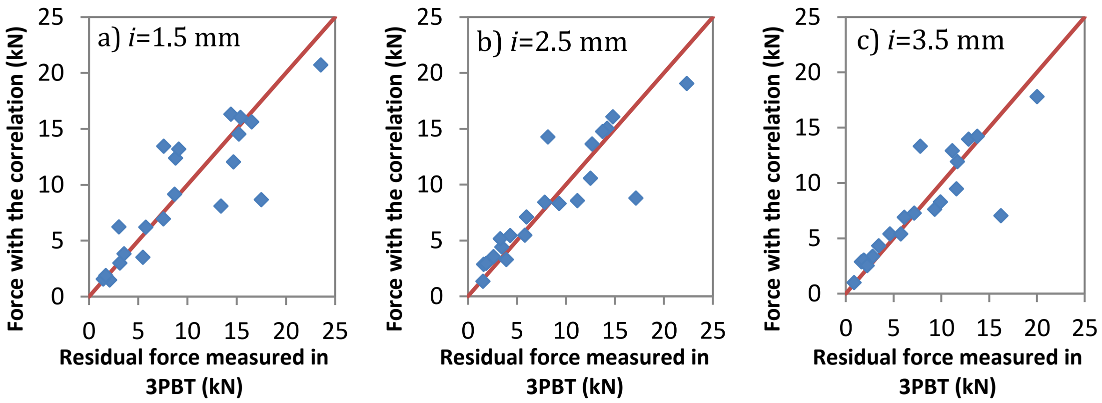

Fig. 10. Comparison between force measured in the 3PBT and force estimated from the BCN results with the correlation.

5.3 Confidence intervals

A natural variability of results should be expected when applying either the 3PBT or the BCN. This variability should also affect the correlations obtained. In certain practical situations, it might be interesting to consider a safety margin capable of compensating at least part of the uncertainty in the prediction of the results of one test. A statistical analysis of the results from Fig. 10 was conducted with the aim of assessing confidence intervals for the correlation proposed.

First, the Kolmogorov-Smirnov test was applied to determine whether the error in the predictions from Eq. 1 with regards to the experimental results follow a normal distribution. Once the normality was verified, the confidence interval of 99% ($CI_{99\%}$) presented in table 4 were calculated for the displacements *i* of 1.5, 2.5 and 3.5 mm. The predicted value of the 3PBT considering the safety margin should be calculated according with Eq. 2.

$$F_{3PBT,i} = a \cdot F_{BCN,i} + b \cdot {E_{BCN,i}}^2 - CI_{99\%,i} \qquad (2)$$

5.4 Verification of the results

The formulation obtained in the parametric study is here compared with the experimental results of the 3PBT for all dosages. Fig. 11 shows several results of the Load-CMOD for both the experimental data (3PBT) in a solid line and the results calculated by means of the correlation proposed (Cor) in a dashed line. The points of the predicted results are shown as a continuous plot load-CMOD in combination with the lower confidence interval corresponding to each CMOD.

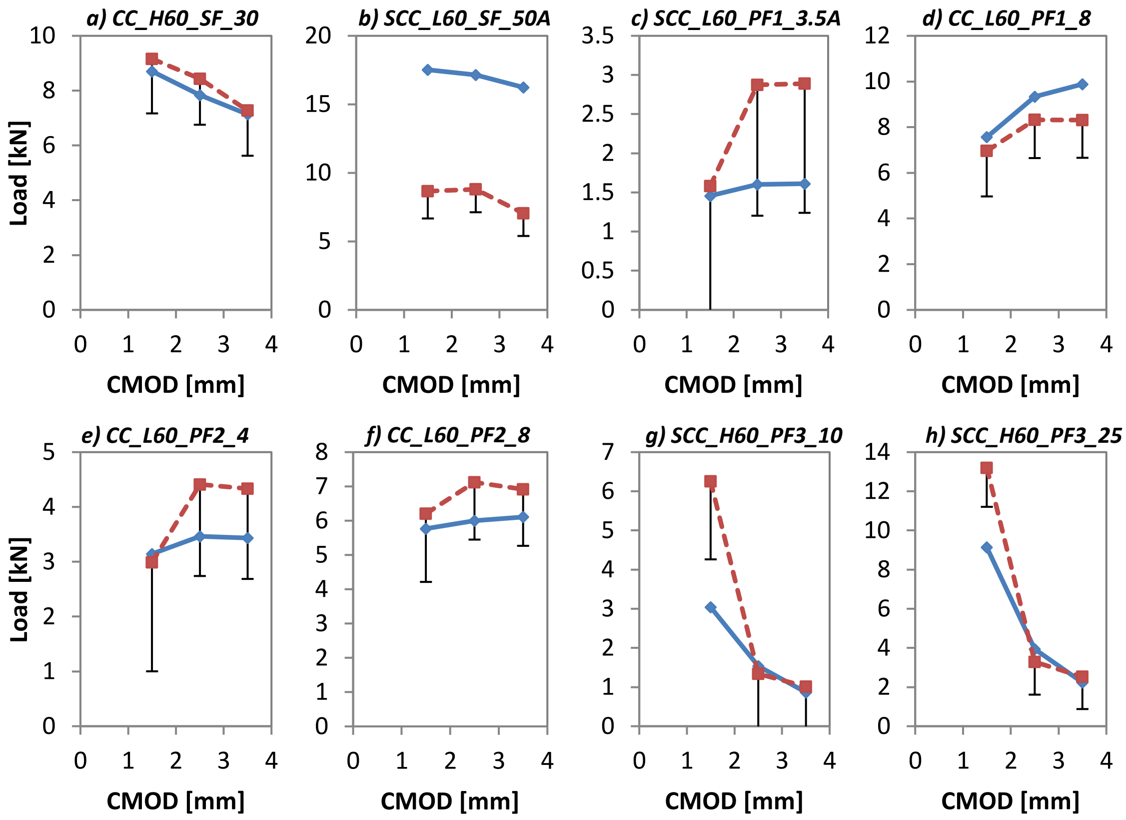

Fig. 11. Real and predicted curves of 3PBT with confidence intervals.

A general overview of the results shows that the calculated curves follow similar trends to those obtained directly from the 3PBT. In the great majority of cases the values measured during the 3PBT are found above the limit defined by the confidence intervals. The only composition in which this is not fulfilled for all displacements is the SCC_H60_SF_60. This confirms that the safety margin introduced is capable of compensating the errors of the predictions.

The accuracy of the prediction decreases with the load level. In certain cases, negative values of the confidence lower limit are obtained. This should be expected when the force measured during the 3PBT are below 5 kN, being especially evident in some of the mixes with plastic fibres.

6 CONCLUSIONS

The approach proposed in this study showed that it is possible to predict the 3PBT based on the results of the BCN with a confidence margin, despite the wide variety of fibre type, fibre content and rheology considered. This opens up the possibility of using the BCN as a complementary test for the systematic quality control of FRC. The same approach may be applied to correlate other tests or to obtain better correlations for specific types of FRC. The following conclusions may be derived based on the results and the analysis presented here.

- The same FRC mix may present hardening in the 3PBT and softening in the BCN. This difference is mainly attributed to the cracking mechanism that takes place in each test. In the BCN, the cracks form abruptly. The load resisted by the cementitious matrix is almost instantaneously transferred to the fibre. Conversely, in the 3PBT the crack height tends to increase progressively, yielding a more gradual load transfer from the matrix to the fibres in the area subjected to tension.
- The correlation between the 3PBT and the BCN considering only one parameter of each test did not provide acceptable results. In order to improve the correlation degree, it is advisable to include more than one parameter in the regression. In the present study, the parameters that yielded the best fits were the force and the energy measured for a certain axial displacement in the BCN, which are related with the force measured in the 3PBT.

- Only one equation (Eq. 2) is needed to correlate the 3PBT and the BCN, regardless of the type of fibre, the content of fibre or the rheology of concrete. The correlation degrees (R^2) achieved range from 0.70 and 0.75 depending on the CMOD. It is important to remark that for low CMOD values, the correlation with the BCN may not be possible due to the differences in terms of the crack formation in both tests.
- Almost all experimental measurements with the 3PBT remain above the prediction with the confidence interval using the results from the BCN. This confirm that the use of confidence intervals is an interesting approach to obtain prediction on the safe side for a material subjected to significant scatter, such as FRC.

ACKNOWLEDGEMENTS

The authors wish to express their gratitude to the Spanish Ministry of Economy and Competitiveness for the financial support in the scope of the project DURADOV (reference: RTC-2015-3617-4). The first author also thanks the Spanish Ministry of Education, Culture and Sport for the FPU13/04864 grant.

REFERENCES

[1] Cavalaro SHP, Aguado A. Intrinsic scatter of FRC: an alternative philosophy to estimate characteristic values. Mater Struct 2015;48(11):3537–3555.

[2] CEN (European Committee for Standardization). EN 14651:2007: Test method for metallic fibre concrete. Measuring the flexural tensile strength (limit of proportionality (LOP), residual). Brussels, 2007.

[3] Parmentier B, Grove E De. Dispersion of the mechanical properties of FRC investigated by different bending tests. Tailor Made Concr. Struct 2008.

[4] Molins C, Aguado A, Saludes S. Double Punch Test to control the energy dissipation in tension of FRC (Barcelona test). Mater Struct 2008;42(4):415-425.

[5] NBN (Bureau de Normalisation). B 15-238. Test on fibre reinforced concrete - bending test on prismatic samples. Norme Belge, Institut Belge de Normalisation, Brussels 1992.

[6] Löfgren I, Stang H, Olesen JF. Fracture Properties of FRC Determined through Inverse Analysis of Wedge Splitting and Three-Point Bending Tests. J Adv Concr Technol 2005;63(3):423-434.

[7] Prisco M, Lamperti MGL, Lapolla S. Double-edge wedge splitting test: preliminary results. In: Fracture Mechanics of Concrete and Concrete Structures (FraMCoS-7). Jeju (S. Korea), 2010. p. 1579–1586.

[8] Prisco M, Ferrara L, Lamperti MGL. Double edge wedge splitting (DEWS): an indirect tension test to identify post-cracking behaviour of fibre reinforced cementitious composites. Mater Struct 2013;46(11):1893–1918.

[9] Model Code 2010. fib Fédération Internationale du Béton, 2010.

[10] Perumal R. Correlation of Compressive Strength and Other Engineering Properties of High-Performance Steel Fiber-Reinforced Concrete. J Mater Civ Eng 2015;27(1):1-8.

[11] Minelli F, Plizzari, G. Fiber reinforced concrete characterization through round panel test - Part I: experimental study. In: Fracture Mechanics of Concrete and Concrete Structures (FraMCoS-7). Jeju (S. Korea), 2010. p. 1451–1460.

[12] Abrishambaf A, Barros JAO, Cunha VMCF. Tensile stress–crack width law for steel fibre reinforced self-compacting concrete obtained from indirect (splitting) tensile tests. Cem Concr Compos 2015;57:153–165.

[13] Minelli F, Plizzari G. Derivation of a simplified stress-crack width law for Fiber Reinforced Concrete through a revised round panel test. Cem Concr Compos 2015;58:95–104.

[14] AENOR (Asociación Española de Normalización y Certificación). UNE 83515. Fibre reinforced concrete. Determination of cracking strength, ductility and residual tensile strength. Barcelona test. Madrid, 2010.

[15] Pujadas P, Blanco A, Cavalaro SHP, de la Fuente A, Aguado A. Multidirectional double punch test to assess the post-cracking behaviour and fibre orientation of FRC. Constr Build Mater 2014;58:214–224.

[16] Pujadas P, Blanco A, Cavalaro S, de la Fuente A, Aguado A. New Analytical Model To Generalize the Barcelona Test Using Axial Displacement. J Civ Eng Manag 2013;19(2):259–271.

[17] Blanco A, Pujadas P, Cavalaro S, de la Fuente A, Aguado A. Constitutive model for fibre reinforced concrete based on the Barcelona test. Cem Concr Compos 2014;53:327–340.

[18] Stähli P, Custer R, Mier JGM. On flow properties, fibre distribution, fibre orientation and flexural behaviour of FRC. Mater Struct 2007;41(1):189–196.

[19] Ferrara L, Ozyurt N, di Prisco M. High mechanical performance of fibre reinforced cementitious composites: the role of 'casting-flow induced' fibre orientation. Mater Struct 2010;44(1):109–128.

[20] Boulekbache B, Hamrat M, Chemrouk M, Amziane S. Flowability of fibre-reinforced concrete and its effect on the mechanical properties of the material. Constr Build Mater 2010;24(9):1664–1671.

[21] Kang ST, Lee BY, Kim JK, Kim YY. The effect of fibre distribution characteristics on the flexural strength of steel fibre-reinforced ultra high strength concrete. Constr Build Mater 2011;25(5):2450–2457.

[22] Zerbino R, Tobes JM, Bossio ME, Giaccio G. On the orientation of fibres in structural members fabricated with self compacting fibre reinforced concrete. Cem Concr Compos 2012;34(2):191–200.

[23] Abrishambaf A, Barros JAO, Cunha VMCF. Relation between fibre distribution and post-cracking behaviour in steel fibre reinforced self-compacting concrete panels. Cem Concr Res 2013;51:57–66.

[24] CEN (European Committee for Standardization). EN 12390-3. Testing hardened concrete. Part 3: Compressive strength of test specimens. Brussels, 2009.

[25] Torrents JM, Blanco A, Pujadas P, Aguado A, Juan-García P, Sánchez-Moragues MA. Inductive method for assessing the amount and orientation of steel fibers in concrete. Mater Struct 2012;45(10):1577–1592.

[26] Cavalaro SHP, López R, Torrents JM, Aguado A. Improved assessment of fibre content and orientation with inductive method in SFRC. Mater Struct 2015;48(6):1859-1873.

[27] Barros JAO, Cunha VMCF, Ribeiro AF, Antunes JAB. Post-cracking behaviour of steel fibre reinforced concrete. Mater Struct 2005;38(1):47–56.

[28] Sivakumar A, Santhanam M. Mechanical properties of high strength concrete reinforced with metallic and non-metallic fibres. Cem Concr Compos 2007;29(8):603–608.

[29] Buratti N, Mazzotti C, Savoia M. Post-cracking behaviour of steel and macro-synthetic fibre-reinforced concretes. Constr Build Mater 2011;25(5):2713–2722.

[30] Soutsos MN, Le TT, Lampropoulos AP. Flexural performance of fibre reinforced concrete made with steel and synthetic fibres. Constr Build Mater 2012;36:704–710.

[31] Alberti MG, Enfedaque A, Gálvez JC. On the mechanical properties and fracture behavior of polyolefin fiber-reinforced self-compacting concrete. Constr Build Mater 2014;55:274–288.

[32] Wille K, El-Tawil S, Naaman AE. Properties of strain hardening ultra high performance fiber reinforced concrete (UHP-FRC) under direct tensile loading. Cem Concr Compos 2014;48:53–66.

[33] Edgington J, Hannant DJ. Steel fibre reinforced concrete. The effect on fibre orientation of compaction by vibration. Mater Struct 1972;5(1):41–44.

[34] Martinie L, Roussel N. Simple tools for fiber orientation prediction in industrial practice. Cem Concr Res 2011;41(10):993–1000.

[35] Wille K, Tue NV, Parra-Montesinos GJ. Fiber distribution and orientation in UHP-FRC beams and their effect on backward analysis. Mater Struct 2013;47(11):1825–1838.

[36] Bernard ES. Correlations in the behaviour of fibre reinforced shotcrete beam and panel specimens. Mater Struct 2002;35(3):156–164.